

# Features of reconstruction of color images of extended objects by pulse holograms

© N.D. Vorzobova, I.V. Krivoschekov, P.P. Sokolov

ITMO University,  
St. Petersburg, Russia  
e-mail: vorzobova@mail.ifmo.ru

Received May 15, 2024

Revised May 15, 2024

Accepted May 29, 2024

The features of combining monochrome components of color images of depth-extended objects reconstructed by transmission pulse holograms in monochromatic light with differences in conditions of holograms recording and image reconstruction are considered. Analytical expressions that allow one to evaluate the degree of alignment in size and depth and numerical assessments of mismatches are given. The advantage of combining monochrome components in depth is shown.

**Keywords:** pulsed holography, color holographic images of extended objects.

DOI: 10.61011/EOS.2024.06.59532.6687-24

## 1. Introduction

Three-dimensional color imaging is one of the most attractive applications of holography. Digital color imaging techniques based on the reconstructed field amplitude and phase calculation followed by display using spatial light modulators [1,2] or printing on recording materials [3,4] have been extensively developed in recent years.

In digital holography, provision of color specifications, necessary horizontal and vertical parallax together with depth imaging requires a large amount of computation. Despite continuous improvement of computational algorithms, there is a problem in reconstructing deeply extended items [5–9]. Therefore, it appears important to focus on analogue techniques that enable imaging of extended items.

In analog color holography, the greatest success has been achieved in making white-light reflection holograms using continuous wave lasers [10–14]. However, when using continuous light, stable recording conditions are required and still holograms can be made.

Pulsed lasers provide a considerable advantage. Pulsed holography has been developed towards making white-light holograms using a two-stage technique [15,16] due to the problems with sensitivity of high-resolution material to pulsed light. This technique is based on making transmission holograms at the first stage and white-light reflection holograms at the second stage. However, white-light reconstruction imposes restriction on image depth.

Extensive development of semiconductor technology and emergence of high-intensity visible light sources provides an opportunity of making large-depth color images reconstructed in monochromatic light by transmission pulsed holograms. The advantage of transmission hologram recording is in the opportunity to reduce the resolution requirements and to use materials sensitive to pulsed light.

Our previous work [17] discussed the special aspects of making images of extended objects to be reconstructed by monochrome transmission pulsed holograms and showed an opportunity to reduce the pulsed laser output energy requirements. This paper will address the aspects of reconstructing color images of extended objects by pulsed holograms.

## 2. Transmission pulsed hologram recording conditions

Transmission holograms were recorded using single-layer materials based on silver halide emulsions made by National Research Center „Kurchatov Institute“ with introduction of optical sensitizers providing wide visible spectral sensitivity, as well as using combination of commercial materials VRP and PFG-01 („Kompaniya Slavich“).

Ruby and neodymium glass frequency-doubled lasers, 693 nm and 530 nm, and stimulated Raman scattering laser [18], 678 nm and 530 nm, with pulse widths of about 10 ns and output energy of 0.2–1 J were used as pulsed light sources.

To avoid „extra“ images, reference beams in the recording geometry were spatially separated. Simple computation performed for recording wavelengths of 678 nm and 530 nm, reconstruction wavelengths of 633 nm, 650 nm and 530, 532 nm, angular extent of an object 40°, an angle of incidence of the 678 nm reference beam of 30° and angular selectivity defined by the end point of an object gives an angle between the reference beams equal to 23–25°.

Dual-wavelength recording provided 405 × 280 mm transmission holograms, including holographic portraits [19,20].

### 3. Aspects of making color images of extended objects

The issue of aligning monochrome components of color images of extended objects with different wavelengths and recording/reconstruction geometry parameters is of utmost interest. Possible differences are, in particular, associated with a tendency to reduce dimensions of monochromatic light fixtures. Let's consider two special cases — provision of equal dimensions of monochrome components or alignment of monochrome components in depth. For the purpose of analysis, the following expressions will be used [21]:

$$V = \left(1 + \frac{z_1}{\mu z_c} - \frac{z_1}{z_r}\right)^{-1}, \quad (1)$$

$$z_3 = \left(\frac{1}{z_c} + \frac{\mu}{z_1} - \frac{\mu}{z_r}\right)^{-1}, \quad (2)$$

where  $V$  is the transverse image magnification,  $z_1$  is the distance from the object to the hologram,  $\mu$  is the reconstructing and recording wavelength ratio,  $z_c$  is the distance from the reconstructing source to the hologram,  $z_r$  is the distance from the reference source to the hologram,  $z_3$  is the distance from the image to the hologram.

#### 3.1. Equality of magnifications of monochrome components of a color image

First let's consider the equality conditions of magnifications (dimensions) of monochrome components with image dimensions equal to object dimensions:

$$V_1 = V_2 = 1. \quad (3)$$

In this case, for reconstructing source positions according to expression (1), the following conditions shall be satisfied:

$$z_{c1} = \frac{z_{r1}}{\mu_1}, \quad (4)$$

$$z_{c2} = \frac{z_{r2}}{\mu_2}. \quad (5)$$

Indices 1 and 2 correspond to „red“ and „green“ components, respectively. Misalignment of components in depth is determined as:

$$\Delta z_3 = z_{31} - z_{32}. \quad (6)$$

Using (2) and substituting (4) and (5) into (6), we find

$$\Delta z_3 = z_1 \left( \frac{1}{\mu_1} - \frac{1}{\mu_2} \right). \quad (7)$$

Now let's consider the case of magnification equality when image dimensions are not equal to object dimensions:

$$V_1 = V_2 \neq 1. \quad (8)$$

We introduce a simplifying condition and assume that the reference sources are at the same distance from the

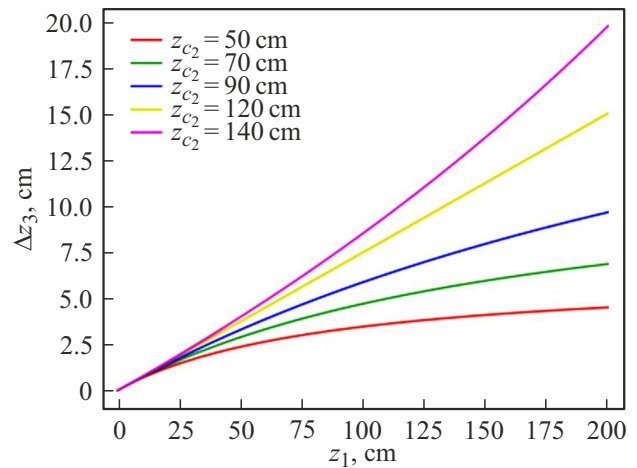


**Figure 1.** Depth misalignment of monochrome components ( $\Delta z_3$ ) vs. the distance to the extended object fragments ( $z_1$ ) for various values of  $z_{c_2}$ . Recording wavelengths are 678 nm and 530 nm, reconstruction wavelengths are 633 nm and 532 nm,  $z_r = 120$  cm.

hologram plane (which generally corresponds to recording conditions):

$$z_{r1} = z_{r2} = z_r. \quad (9)$$

Using (1), the reconstruction source position ratio is calculated:

$$z_{c1} = \frac{\mu_2}{\mu_1} z_{c2}. \quad (10)$$

By substituting (10) into (6), the expression for depth misalignment is derived:

$$\Delta z_3 = \frac{z_{c2} z_1 z_r}{z_1 z_r + \mu_2 z_{c2} (z_r - z_1)} \left( \frac{\mu_2}{\mu_1} - 1 \right). \quad (11)$$

Figure 1 shows the curves of depth misalignment vs. object length for various  $z_{c_2}$ . The curves are plotted for  $z_r = 120$  cm,  $\mu_1 = 633/678$ ,  $\mu_2 = 532/530$ . It can be seen that misalignment of monochrome components in depth increases as the distance to the extended object fragments increases. The increasing distance to the reconstructing sources also leads to growing misalignment, whereby differences in misalignment for near and far fragments decrease as the distance to the reconstructing sources decreases.

Numerical estimates for  $z_{c_2} = 50$  cm are as follows. For near fragments ( $z_1 = 40$  cm), component misalignment in depth is 2 cm, and for far fragments ( $z_1 = 200$  cm), it is 4.5 cm, which can be seen when viewing the images from a typical distance of 50 cm from the hologram.

#### 3.2. Alignment of monochrome component in depth

Alignment of monochrome component in depth is determined by the following condition

$$z_{31} = z_{32}. \quad (12)$$

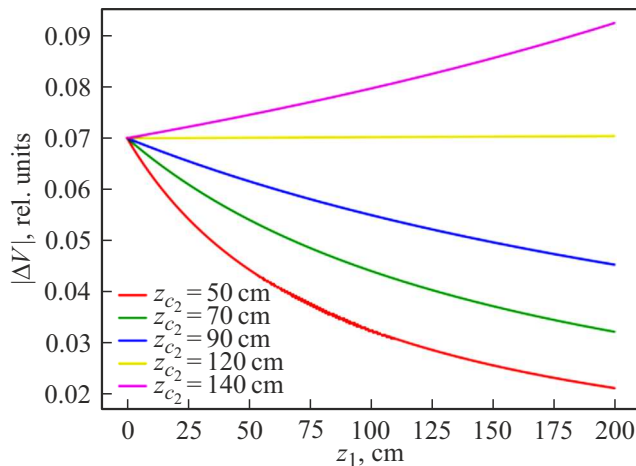


**Figure 2.** Absolute misalignment of monochrome components ( $\Delta V$ ) by magnification vs. the distance to the extended object fragments ( $z_1$ ) for various  $z_{c_2}$ . Recording wavelengths are 678 nm and 530 nm, reconstruction wavelengths are 633 nm and 532 nm,  $z_r = 120$  cm.

Similar to Section 3.1, when the distances to the reference sources are equal, using equation (2) we find that to satisfy condition (12) the ratio of distances to the reconstructing sources shall meet the following condition

$$z_{c_1} = z_{c_2} \frac{z_1}{z_1 + z_{c_2} [\mu_2 (1 - \frac{z_1}{z_r}) - \mu_1 (1 - \frac{z_1}{z_r})]}. \quad (13)$$

Misalignment by magnification is calculated as

$$\Delta V = V_1 - V_2. \quad (14)$$

Using (1) and substituting (13) into (14), we find

$$\Delta V = \frac{z_r z_{c_2} (\mu_1 - \mu_2)}{z_1 z_r - \mu_2 z_1 z_{c_2} + \mu_2 z_r z_{c_2}}. \quad (15)$$

Using expression (15), curves of the absolute misalignment by magnification vs. the object length (Figure 2) were plotted for  $z_r = 120$  cm,  $\mu_1 = 633/678$ ,  $\mu_2 = 532/530$ .

For clarity, the curves are shown for the absolute magnification difference because the value of difference (14) will be negative, i.e. the „green“ component size will be always larger than the „red“ component size. The given dependences show that at  $z_c < z_r$  the differences in magnifications (dimensions) of the monochrome components for far fragment of the extended object are smaller than for near fragments, i.e. far fragments will be better aligned. When  $z_c > z_r$ , vice versa, these differences will be larger.

Numerical estimates for  $z_{c_2} = 50$  cm are as follows. For far fragments ( $z_1 = 40$  cm)  $|\Delta V| = 0.05$ , which for the image dimensions  $L_1 = 20$  cm and  $L_2 = 4$  cm corresponds to the dimension difference  $\Delta L_1 = 1$  cm and  $\Delta L_2 = 2$  mm. For far fragments ( $z_1 = 200$  cm)  $|\Delta V| = 0.02$ , which for the same image dimensions corresponds to  $\Delta L_1 = 4$  mm,  $\Delta L_2 = 0.8$  mm, i.e. the differences are much smaller than for near fragments.



**Figure 3.** Fragment of reconstructed color image.

Comparison of the determined misalignments in dimensions of the monochrome components of color images, when they are aligned in depth, with the results obtained in Section 3.1 with equal image dimensions and misalignment in depth, as well as comparison with the eye resolution demonstrate the advantage of the alignment in depth for visual perception.

## 4. Experimental results

The experiments for alignment of the monochrome components of a color image used a  $405 \times 280$  mm hologram recorded on 678 nm and 530 nm. Images were reconstructed using the 633 nm (helium-neon laser), 650 nm (semiconductor laser module) and 532 nm (SDL 303 laser pointer) light.

Figure 3 shows the photo of a color image fragment reconstructed at 633 nm and 532 nm. Alignment of monochrome components in depth is provided in the reconstructed image. Mismatch in dimensions (red carnation) of about 2 mm with a larger size of the „green“ components can be seen, which agrees with the calculation results in Section 3.2.

When viewing from a distance of 50 cm from the hologram, this value is comparable with the eye resolution. Moreover, it can be seen that, for a farther object (white carnation), mismatch in dimensions is smaller.

For full alignment of monochrome components, according to expressions (11) and (15), the following conditions shall be satisfied

$$\mu_1 = \mu_2. \quad (16)$$

Conditions (16) can be essentially satisfied taking into account a wide range of monochromatic light sources based on LED and laser diodes. However, the light sources with alignment in depth used in this study, provide images of

color objects and humans with quite good characteristics for visual perception.

## 5. Conclusion

The paper discusses the aspects of alignment of the monochrome components of color images of deeply extended objects reconstructed by transmission holograms with the difference in hologram recording and image reconstruction conditions. Analytical expressions for two cases have been obtained — misalignment in depth with equal image dimensions and alignment in depth with misalignment by image dimensions. Quantitative evaluations of misalignments have been made for dual-wavelength pulsed light recording and the advantage of alignment in depth has been shown. The findings may be also applicable to three-wavelength recording.

The findings are of interest for making pulsed and continuous laser transmission holograms and for monochromatic reconstruction of images using analog and analog-digital techniques. The findings may be also useful for the development of compact light fixtures based on modern monochromatic light sources.

## Conflict of interest

The authors declare that they have no conflict of interest.

## References

- [1] S.-F. Lin, H.-K. Cao, E.-S. Kim. *Opt. Express*, **27** (11), 15926 (2019). DOI: 10.1364/OE.27.015926
- [2] H.-G. Choo, T. Kozacki, W. Zaperty, M. Chlipala, Y. Lim, J. Kim. *Appl. Opt.*, **58** (34), G96 (2019). DOI: 10.1364/AO.58.000G96
- [3] P. Gentet, M. Coffin, Y. Gentet, S.-H. Lee. *Appl. Sci.*, **13**, 12289 (2023). DOI: 10.3390/app132212289
- [4] A.F. Smyk, A.V. Shurygin, S.B. Odinkov, A.N. Putilin. *J. Opt. Techn.*, **89** (3), 151 (2022). DOI: 10.1364/JOT.89.000151
- [5] Y. Zhao, J.-W. Bu, W. Liu, J.-H. Uji, Q.-H. Yang, S.-F. Lin. *Opt. Express*, **31** (2), 1641 (2023). DOI: 10.1364/OE.477666
- [6] J. Zhao, Z. Gao, S. Wang, Yu. Niu, L. Deng, Y. Sa. *Appl. Sci.*, **13**, 11430 (2023). DOI: 10.3390/app132011430
- [7] K. Matsushima, N. Sonobe. *Appl. Opt.*, **57** (1), A150 (2018). DOI: 10.1364/AO.57.00A150
- [8] P. Su, Q.-X. Gao, Z.-H. He, J.-S. Ma. *Optik*, **200**, 163044 (2020). DOI: 10.1016/j.ijleo.2019.163044
- [9] J. Behal, P. Memmolo, L. Miccio, V. Bianco, P. Ferraro. *Opt. Laser Techn.*, **170**, 110286 (2024). DOI: 10.1016/j.optlastec.2019.105590
- [10] H. Bjelkhagen, D. Brotherton-Ratcliffe. *Ultra Realistic Imaging Advanced Techniques in Analogue and Digital Colour Holography* (Taylor & Francis Group, London, N.Y., 2013).
- [11] V. Martín, Ju. Marín-Saez, M. Gomez-Climente, D. Chemisana, M.-V. Collados, J. Atencia. *Opt. Laser Techn.*, **143**, 107303 (2021). DOI: 10.1016/j.optlastec.2021.107303
- [12] H.I. Bjelkhagen, E. Mirlis. *Appl. Opt.*, **47** (4), A123 (2008). DOI: 10.1364/ao.47.00a123
- [13] P. Gentet, Y. Gentet, P.H. Choi, S.H. Lee. *Open Physics*, **17** (1), 449 (2019). DOI: 10.1515/phys-2019-0046
- [14] V.V. Shelkovnikov, D.I. Derevyanko, E.F. Pen. *Opt. and Spectr.*, **130** (10), 1559 (2022). DOI: 10.21883/os.2022.10.53626.3795-22
- [15] E.F. Artemiev, V.G. Bespalov, V.Z. Bryskin, N.D. Vorzobova, M.M. Ermolaev, D.I. Stasel'ko. V sb.: *Opticheskaya golografiya. Prakticheskoe primenenie* (Nauka, L., 1985), s. 107. (in Russian)
- [16] N.D. Vorzobova. V sb.: *Golografiya: fundamental'nye issledovaniya, innovatsionnye proekty i nanotekhnologii. Materialy XXVI shkoly po kogerentnoy optike i golografii* (Papyrus, Irkutsk, 2008), p. 175 (in Russian).
- [17] N.D. Vorzobova., P.P. Sokolov. *Opt. Spectrosc.*, **129** (3), 309 (2021). DOI: 10.21883/OS.2021.03.50658.251-20
- [18] V.G. Bespalov, V.N. Krylov, V.N. Mikhailov, V.A. Parfenov, D.I. Staselko. *Opt. Spectrosc.*, **70** (2), 193 (1991).
- [19] N.D. Vorzobova, R.V. Ryabova. In: *Proceedings of 10th International Symposium on Display Holography*, 2015, p. 146.
- [20] N.D. Vorzobova, V.N. Sizov, R.V. Rjabova. In: *Three-Dimensional Holography: Science, Culture, Education*, 1991, vol. 1238, p. 462. DOI: 10.1117/12.19387
- [21] R.I. Collier, C.B. Burckhart. L.H. Lin. *Optical Holography* (Bell Telephone Laboratories, Murray Hill, New Jersey; Academic Press, New York and London, 1971), 605 p.

Translated by E.Illinskaya